Photoredox Properties of $[OsN(NH_3)_4]^{3+}$ and Mechanism of Formation of $[\{Os(NH_3)_4(CH_3CN)\}_2N_2]^{5+}$ through a Nitrido-coupling Reaction

Hon-Wah Lam, Chi-Ming Che* and Kwok-Yin Wong
Department of Chemistry, University of Hong Kong, Pokfulam Road, Hong Kong

The oxidation of $[Os(NH_3)_5Cl]^{2+}$ by Ce^{IV} in water gave $[OsN(NH_3)_4]^{3+}$ quantitatively. Excitation of $[OsN(NH_3)_4]^{3+}$ in the solid state or in solution at 300–400 nm resulted in room-temperature photoluminescence. The low-lying spin orbital E sublevel of the $^3E\ \{^3[(d_{xy})^1(d_{\pi}{}^*)^1]\}$ state was assigned as the emission state. The excited state of $[OsN(NH_3)_4]^{3+}$ was quenched by electron donors such as aromatic hydrocarbons, alkoxybenzenes, amines and alcohols. A photoinduced electron-transfer mechanism is proposed for the quenching processes. The emission lifetime of $[OsN(NH_3)_4]^{3+}$ depended on the complex concentration. An excited-state bimolecular self-quenching mechanism ($[Os^{VI}{\equiv}N]^* + [Os^{VI}{\equiv}N] \longrightarrow$ product) is likely. Photolysis of $[OsN(NH_3)_4]^{3+}$ in the presence of an electron donor such as 1,4-dimethoxybenzene or C_6Me_6 in acetonitrile led to the formation of the μ-dinitrogen product $[\{Os(NH_3)_4(CH_3CN)\}_2N_2]^{5+}$. The coupling reaction obeyed the kinetics rate = $k_2[Os^{VI}][Os^{V}]$ where k_2 was estimated to be $(3.75 \pm 0.30) \times 10^5$ dm³ mol⁻¹ s⁻¹ at 298 K. Oxidation of $[\{Os(NH_3)_4(CH_3CN)\}_2N_2]^{5+}$ by Ce^{IV} in water followed by precipitation with 2 mol dm⁻³ HCl gave the product $[OsN(NH_3)_4]Cl_3$ in detectable yield.

The photophysical properties and photochemistry of d^2 metal oxo (M=O) and nitrido (M≡N) complexes have received considerable attention because these classes of complexes are usually photoluminescent and have long-lived electronic excited states.[1–4] Population of an electron in the lowest-lying d_{π^*} orbital ($d_{\pi^*} = d_{xz}, d_{yz}$) through photoexcitation is expected to weaken the metal–ligand multiple bond. Thus these complexes, if suitably designed, are suggested to be versatile reagents for photoinduced atom-transfer reactions. The success in the demonstration of photoinduced oxidation of alcohols, alkenes and triphenylphosphine by *trans*-dioxo(macrocyclic tertiary amine)osmium(VI) complexes[2] has led us to investigate the photophysical and photochemical properties of the isoelectronic osmium(VI) nitrido system. Our interest in d^2 Os≡N complexes is also due to their luminescent properties[4] as well as their possible application in modelling the nitrogen fixation reaction. Part of this work has previously been communicated.[1a,c]

Experimental

Materials.—Sodium hexachloroosmate(IV) was purchased from Johnson Matthey. Tetrabutylammonium hexafluorophosphate and perchlorate (Southwestern Analytical Chemicals) were dried under vacuum at 60 °C for 48 h before use. Acetonitrile (Ajax AR) was distilled over CaH_2. Dichloromethane (Ajax AR) was purified by washing with concentrated H_2SO_4 followed by 5% aqueous Na_2CO_3 and distilled over P_2O_5. Deionized water was doubly distilled over alkaline potassium permanganate. Organic substrates used in quenching experiments were purified according to literature procedures.[5] All other chemicals were analytical grade used without further purification.

Measurements.—The UV/VIS spectra were obtained on a Shimadzu UV-240 spectrophotometer, infrared spectra as Nujol mulls on a Nicolet 20-FXC FT-IR spectrophotometer. Steady-state emission spectra were recorded on a Hitachi 650-60 fluorescence spectrophotometer. Corrected emission spectra were obtained using a Hitachi 650-0178 data processor accessory. The absolute luminescence quantum yield was measured by the method of Demas and Crosby[6] using quinine sulfate in 0.05 mol dm⁻³ sulfuric acid as standard. Sample and standard solutions were thoroughly degassed with no fewer than three freeze–pump–thaw cycles.

Luminescence lifetimes of solid and solution samples were measured using a Spectra-Physics DCR-3 Nd:YAG pulsed laser system. Unless otherwise stated, the excitation light source was at 355 nm. The emission intensity decay data were processed using a modified version of the Tektronix GURU II program on an Epson PCe microcomputer.

Cyclic voltammetry was performed using a Princeton Applied Research (PAR) model 175 universal programmer, model 173 potentiostate and model 179 digital coulometer. A conventional two-compartment cell was used. The working electrodes were either glassy carbon (Atomergic Chemetals V25) or pyrolytic graphite (Union Carbide). Controlled-potential coulometry was performed by a PAR model 377A coulometric cell system. Elemental analyses were by Butterworth Laboratory.

Preparations.—The complex $[Os(NH_3)_5Cl]Cl_2$ was prepared by the literature method.[7]

$[OsN(NH_3)_4]Cl_3$. A mixture of $[NH_4]_2[Ce(NO_3)_6]$ (1.0 g) and $[Os(NH_3)_5Cl]Cl_2$ (0.5 g) in deionized water (50 cm³) was stirred at room temperature for 15 min. Addition of concentrated HCl (3 cm³) to the resulting solution gave $[OsN(NH_3)_4]Cl_3$ as a yellow precipitate. The crude product was collected by filtration and washed with 2 mol dm⁻³ HCl, methanol and diethyl ether. A microcrystalline solid was obtained by recrystallization from hot 2 mol dm⁻³ HCl (yield *ca.* 50%) (Found: H, 3.30; Cl, 28.10; N, 19.05. Calc.: H, 3.15; Cl, 28.05; N, 18.85%). UV/VIS [λ_{max}/nm (ε/dm³ mol⁻¹ cm⁻¹) in 0.1 mol dm⁻³ CF_3CO_2H]: 362 (90) and *ca.* 240 (*ca.* 1300).

$[OsN(NH_3)_4][CF_3SO_3]_3$. A solution of $[OsN(NH_3)_4]Cl_3$ (0.1 g) in trifluoromethanesulfonic acid (2 cm³) was stirred under argon to give a pale yellow solution. Upon addition of diethyl ether, yellow solid $[OsN(NH_3)_4][CF_3SO_3]_3$ was precipitated. The product was collected by filtration, washed with diethyl ether and dried under vacuum (yield *ca.* 90%) (Found: C, 5.15; H, 1.65; N, 9.85. Calc.: C, 5.00; H, 1.65; N, 9.75%). UV/VIS [λ_{max}/nm (ε/dm³ mol⁻¹ cm⁻¹) in CH_3CN]: 400 (150), 320 (80), 270 (260) and 215 (1300).

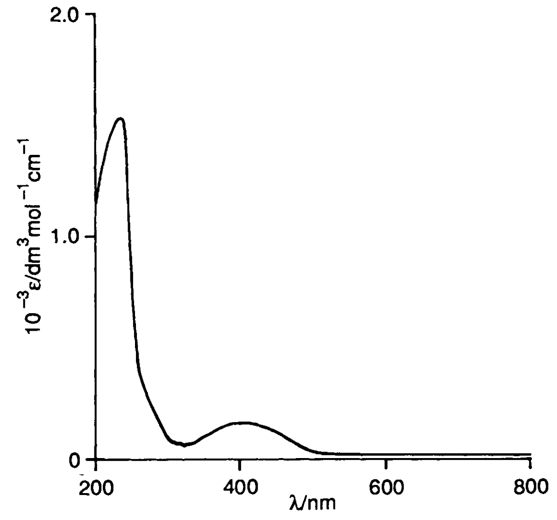

Fig. 1 The UV/VIS spectrum of $[OsN(NH_3)_4][CF_3SO_3]_3$ in acetonitrile

Table 1 Emission spectral data for $[OsN(NH_3)_4][CF_3SO_3]_3$ at 298 K

Medium	Emission λ/nm (lifetime/μs)
Solid	610 (1.40)
Acetonitrile	545 (1.56)[a]
Methanol	520 (0.60)[b]
Water	520 (0.10)[b]
D_2O	520 (0.40)[b]

[a] Lifetime measured at infinite dilution. [b] Lifetime measured at concentration 1.30 × 10^{-3} mol dm^{-3}.

Results and Discussion

The oxidative deprotonation of $[Os(NH_3)_5Cl]^{2+}$ in aqueous solution to give $[OsN(NH_3)_4]^{3+}$ has previously been studied by Taube and co-workers.[7] A mechanism involving disproportionation of a $[Os(NH_2)(NH_3)_4Cl]^{2+}$ intermediate was proposed. In this work complete oxidation of $[Os(NH_3)_5Cl]^{2+}$ to $[OsN(NH_3)_4]^{3+}$, which was isolated in a pure form by precipitation with HCl, was found to be effected by excess of Ce^{IV}. From the UV/VIS spectrum the $[OsN(NH_3)_4]Cl_3$ prepared by this method was free from the starting material and *trans*-$[Os(NH_3)_4O_2]Cl_2$.[8] As expected, $[OsN(NH_3)_4]Cl_3$ is diamagnetic and displays an intense IR band at 1090 cm^{-1} assignable to $\nu(Os{\equiv}N)$. The structure of $[OsN(NH_3)_4]Cl_3$ is also inferred from the X-ray crystal structure of the coupling product $[\{Os(NH_3)_4(CH_3CN)\}_2N_2]^{5+}$ described in a previous communication.[1c]

Spectroscopic Properties.—The UV/VIS spectrum of $[OsN(NH_3)_4][CF_3SO_3]_3$ in acetonitrile is shown in Fig. 1. Three absorption bands at 270, 300 and 400 nm respectively are observed. With reference to previous work[8] the energy of the d orbitals of $[OsN(NH_3)_4]^{3+}$ are in the order $b_2(d_{xy}) < e(d_{xz},d_{yz}) < b_1(d_{x^2-y^2}) < a_1(d_{z^2})$. The absorption bands in the region 290–400 nm are likely due to the spin-allowed $^1[(d_{xy})^2] \longrightarrow {}^1[(d_{xy})^1(d_{\pi^*})^1]$ ($^1A \longrightarrow {}^1E$) and spin-forbidden $^3[(d_{xy})^1(d_{\pi^*})^1]$ ($^1A \longrightarrow {}^3E$) transitions respectively. The band at 270 nm because of its large absorption coefficient is likely to be the $p_\pi(N^{3-}) \longrightarrow (d_{\pi^*})$ charge-transfer transition.

Excitation of $[OsN(NH_3)_4]^{3+}$ in the solid state or in solution at 300–400 nm resulted in visible room-temperature photoluminescence. Table 1 lists the emission spectral data of $[OsN(NH_3)_4][CF_3SO_3]_3$ in different solvents and in the solid state. The large difference in emission and lowest-allowed absorption energies and the long emission lifetime suggest that the transition involved is a spin-forbidden process. The low-lying spin orbital E sublevel of the ^3E state $^3[(d_{xy})^1(d_{\pi^*})^1]$ is most likely to be the emission state. Fig. 2 shows the emission spectrum of a solid sample of $[OsN(NH_3)_4]Cl_3$ recorded at 77 K, which reveals a vibrational progression of *ca.* 1000 cm^{-1} and E_{0-0} emission energy at *ca.* 2.4 eV (*ca.* 3.8 × 10^{-19} J). This vibrational spacing is close to the $\nu(Os{\equiv}N)$ stretch in the ground state, and is in accord with the molecular orbital diagram proposed by Gray and co-workers[4,8] where the electronic transition $^1A \longrightarrow E$ (^1E,^3E) is vibronically coupled to the $Os{\equiv}N$ stretching for a metal nitrido complex having C_{4v} symmetry. The emission lifetime decreases from acetonitrile to methanol and water. Proton addition was found to quench both the lifetime and intensity of the emission. From the emission lifetime in water and in D_2O at a fixed concentration of the metal complex the kinetic isotope effect for the quenching is 4. It is likely that the interaction of the $Os{\equiv}N$ moiety with the OH group of the solvent may provide an efficient relaxation pathway for the excited state. The luminescence quantum yield of $[OsN(NH_3)_4]^{3+}$ in acetonitrile is estimated to be 0.14 using quinine sulfate as standard with 355 nm excitation.

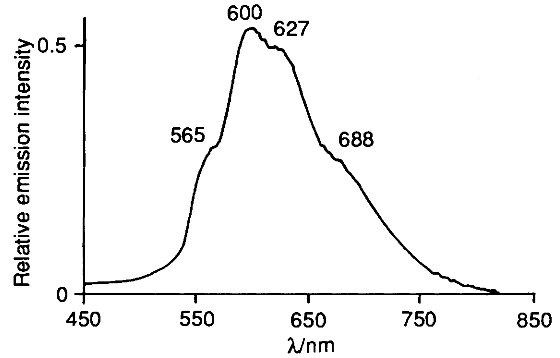

Fig. 2 Emission spectrum of a solid sample of $[OsN(NH_3)_4]Cl_3$ recorded at 77 K

Table 2 Concentration dependence of the emission lifetimes of $[OsN(NH_3)_4][CF_3SO_3]_3$ in 0.1 mol dm^{-3} tetraethylammonium perchlorate–acetonitrile at 298 K

Concentration/ mol dm^{-3}	τ/μs
2.50 × 10^{-4}	1.45
4.44 × 10^{-4}	1.30
5.56 × 10^{-4}	1.31
6.94 × 10^{-4}	1.25
9.17 × 10^{-4}	1.18
1.22 × 10^{-3}	1.07
1.61 × 10^{-3}	1.01
2.44 × 10^{-3}	0.84

The emission lifetime has been found to depend on the concentration of $[OsN(NH_3)_4]^{3+}$. The data are listed in Table 2. As the absorption spectrum of $[OsN(NH_3)_4]^{3+}$ does not show any observable dependence on its concentration, such behaviour is not likely to be a ground-state phenomenon. The relationship between the emission lifetime and the concentration of $[OsN(NH_3)_4]^{3+}$ was found to obey the Stern–Volmer equation (1). An excited-state bimolecular self-quenching

$$1/\tau = 1/\tau_0 + k_{self}[Os{\equiv}N] \qquad (1)$$

mechanism is therefore likely to take place [equation (2)] where k_{self} is the self-quenching rate constant.

$$[Os{\equiv}N]^* + [Os{\equiv}N] \xrightarrow{k_{self}} \text{product} \qquad (2)$$

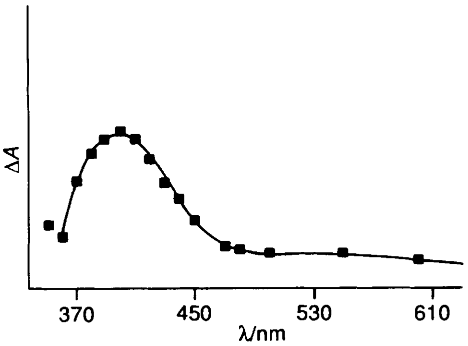

Fig. 3 Transient optical difference spectrum recorded 5 μs after 355 nm laser excitation of $[\mathrm{OsN(NH_3)_4}]^{3+}$ (*ca.* 10^{-3} mol $\mathrm{dm^{-3}}$) and pentamethylbenzene (*ca.* 10^{-3} mol $\mathrm{dm^{-3}}$) in degassed acetonitrile

Table 3 Rate constants for the quenching of $[\mathrm{OsN(NH_3)_4}]^{3+*,a}$ by organic quenchers at 298 K

Quencher	$E_p(\mathrm{Q}^{+/0})^b$/ V *vs.* NHE	k_q/$\mathrm{dm^3\ mol^{-1}\ s^{-1}}$
N,*N*,*N*′,*N*′-Tetramethyl-*p*-phenylenediamine	0.34	6.33×10^9
Phenothiazine	0.77	8.27×10^9
Diphenylamine	1.07	2.13×10^9
Triphenylamine	1.10	1.54×10^9
1,2,4-Trimethoxybenzene	1.36	2.91×10^9
Aniline	1.52	1.27×10^9
1,4-Dimethoxybenzene	1.58	5.66×10^7
Hexamethylbenzene	1.82	7.49×10^7
Pentamethylbenzene	1.95	4.41×10^7
1,2,4,5-Tetramethylbenzene	2.03	1.19×10^7
1,2,4-Trimethylbenzene	2.13	2.38×10^6
1,2,3-Trimethylbenzene	2.23	0.40×10^6
p-Cymene	2.29	0.64×10^6
p-Xylene	2.30	0.44×10^6
Mesitylene	2.35	0.36×10^6
m-Xylene	2.38	0.25×10^6
Cumene	2.53	0.15×10^6
Toluene	2.64	0.14×10^6
Styrene	2.75	1.41×10^6

[a] 1 mmol $\mathrm{dm^{-3}}$ $[\mathrm{OsN(NH_3)_4}][\mathrm{CF_3SO_3}]_3$ in degassed acetonitrile. [b] Ref. 11.

From the bonding scheme, the chemistry of d^2 metal nitrido complexes in C_{4v} symmetry is dominated by the $\mathrm{a_1(d_{z^2})}$ σ^* antibonding orbital.[9,10] Because of metal–nitrogen bonding, the $\mathrm{e(d_{xz},d_{yz})}$ orbitals are antibonding in nature. Excitation of the $\mathrm{b_1}$ (d_{xy}) electron to the e $(\mathrm{d_{xz},d_{yz}})$ orbital will thus lead to a weakening of the Os≡N bond and increase the nucleophilicity of the nitrido ligand. In the absence of other quenchers, the excited $[\mathrm{Os^{VI}{\equiv}N}]$ complex may interact with its ground state which has an electrophilic moiety.

Hoffman and co-workers[10] have studied the mechanism of interaction between two M≡N units. According to their work, such interaction should be most favourable for late transition metals as the nitrogen component of the acceptor orbital is the largest. From their molecular orbital calculation on $[\mathrm{Mo(N)Cl_4}]^-$ two orientations for the bimolecular interaction are possible: the head-on interaction (M≡N ··· N≡M) and the head-to-tail interaction (M≡N ··· M≡N). Since the excited state of the six-co-ordinated $[\mathrm{OsN(CN)_5}]^{2-}$ complex also exhibits similar self-quenching phenomena,[1b] interaction *via* head-on coupling of two nitrido units is therefore the most probable mechanism [equation (3)]. In this work, the observed large self-

$$[\mathrm{Os{\equiv}N}]^* + [\mathrm{Os{\equiv}N}] \longrightarrow [\mathrm{Os{\equiv}N \cdots N{\equiv}Os}] \qquad (3)$$

quenching rate of the photoluminescence can be attributed to the interaction between the [Os≡N] units in the ground and excited states.

Electrochemistry and Estimation of the Excited-state Reduction Potential.—The cyclic voltammogram of $[\mathrm{OsN(NH_3)_4}][\mathrm{CF_3SO_3}]_3$ in acetonitrile displays an irreversible reduction wave at −0.63 V *vs.* $[\mathrm{Fe(\eta\text{-}C_5H_5)_2}]^{+/0}$ [0.23 V *vs.* normal hydrogen electrode (NHE)]. Controlled-potential coulometry established $n = 1.0$ for the reduction wave. Although the $\mathrm{Os^{VI}}$–$\mathrm{Os^{V}}$ couple is irreversible, the potential of the reduction wave can be taken as the upper limit of $E^\circ(\mathrm{Os^{VI}\text{–}Os^{V}})$. The excited-state redox potential of $[\mathrm{OsN(NH_3)_4}]^{3+*}$ can be estimated from equation (4) where $E^{\circ*}(\mathrm{Os^{VI}\text{–}Os^{V}})$ and $E^\circ(\mathrm{Os^{VI}\text{–}Os^{V}})$ are the standard reduction potentials in the excited and ground states respectively and E_{0-0} is the zero–zero emission energy.

$$E^{\circ*}(\mathrm{Os^{VI}\text{–}Os^{V}}) = E^\circ(\mathrm{Os^{VI}\text{–}Os^{V}}) + E_{0-0} \qquad (4)$$

The estimated excited-state redox potential of $[\mathrm{OsN(NH_3)_4}]^{3+}$ is, therefore, 2.2 V *vs.* NHE taking E_{0-0} to the emission maximum which is 2.4 eV from the emission spectrum measured at 30 K.

Photoinduced Electron-transfer Reactions.—The $^3[\mathrm{d}_{xy},\mathrm{d}_{\pi^*}]$ excited state of $[\mathrm{OsN(NH_3)_4}]^{3+}$ was found to be quenched by various electron donors such as aromatic hydrocarbons, alkoxybenzenes, olefins and amines. Quenching by energy transfer should not be the major pathway as the triplet-state energies of the quenchers chosen are high compared to the excited-state energies of the metal complexes. Table 3 lists the quenching rate constants for some organic substrates.

For the quenching of $[\mathrm{OsN(NH_3)_4}]^{3+*}$ by substituted toluenes, a linear Hammett plot with a slope, ρ, of −7.3 is obtained. Such a large negative ρ value implies the development of full positive charge in the transition state, suggesting a charge-transfer mechanism is taking place. Fig. 3 shows the transient optical difference (Δ*A*) spectrum recorded 5 μs after flashing an acetonitrile solution of $[\mathrm{OsN(NH_3)_4}]^{3+}$ and pentamethylbenzene at 355 nm. The absorption peak at *ca.* 400 nm is due to the formation of cation radicals of pentamethylbenzene. The photochemically generated cation radical would react *via* back electron transfer or other pathways as shown by the decay of the absorption signal eventually to the background level. Similar observations were made upon flashing a degassed acetonitrile solution of $[\mathrm{OsN(NH_3)_4}]^{3+}$ in the presence of 1,4-dimethoxybenzene. From these studies an electron-transfer mechanism in equation (5) can be proposed for the quenching reaction.

(5)

For the quenching by amines the rate constants fall in the order: *N*,*N*,*N*′,*N*′-tetramethyl-*p*-phenylenediamine > phenothiazine > diphenylamine > triphenylamine > *N*-methylaniline > aniline, which is also the order of increasing oxidation potential of these amines. This indicates a charge-transfer mechanism for the quenching process.

Fig. 4 shows a non-linear least-squares plot of *RT*ln k_q *vs.* E° for the quenching of $[\mathrm{OsN(NH_3)_4}]^{3+*}$ by a series of atomic hydrocarbons. An Arrhenius linear region with slope close to −0.5 at low exoergicity is followed by a plateau region at high exoergicity.[12] The excited-state redox potential of $[\mathrm{OsN(NH_3)_4}]^{3+*}$ is estimated to be 2.2 V *vs.* NHE[12] which agrees with that deduced from spectroscopic and electrochemical measurements. The limiting rate constant of the quenching of $[\mathrm{OsN(NH_3)_4}]^{3+*}$ by aromatic hydrocarbons was found to be an order of magnitude smaller than the calculated diffusion-limited rate constant. The non-adiabaticity of the electron transfer could be the cause of the observed phenomenon.

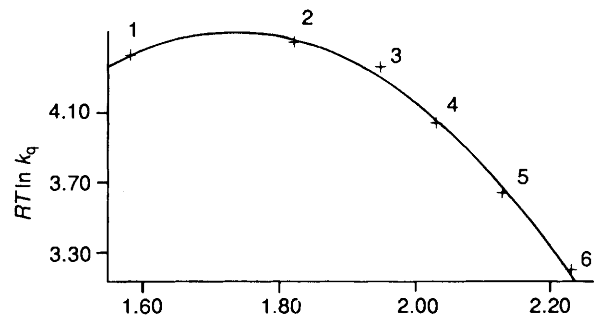

Fig. 4 Non-linear least-squares plots of $RT\ln k_q$ *vs.* $E°$ for the quenching of $[OsN(NH_3)_4]^{3+}$ by some aromatic hydrocarbons in acetonitrile at 298 K: 1, 1,4-dimethoxybenzene; 2, C_6Me_6; 3, C_6HMe_5; 4, 1,2,4,5-tetramethylbenzene; 5, 1,2,4-trimethylbenzene; 6, 1,2,3-trimethylbenzene

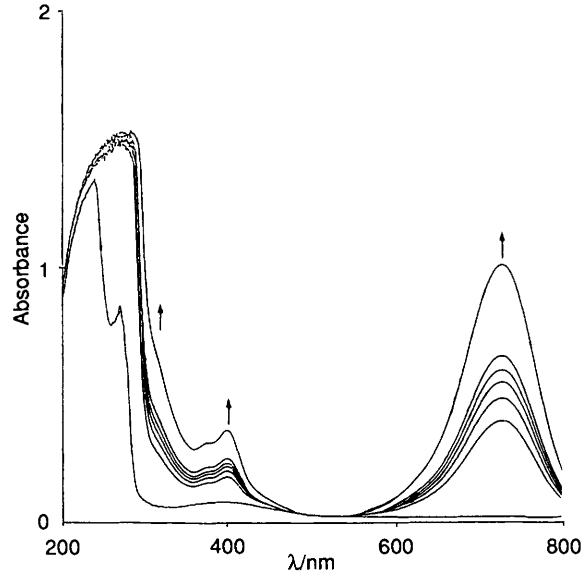

Fig. 5 The UV/VIS spectral changes for the photochemical reaction between $[OsN(NH_3)_4]^{3+}$ (*ca.* 10^{-3} mol dm^{-3}) and hexamethylbenzene (*ca.* 10^{-3} mol dm^{-3}) in degassed acetonitrile at 298 K

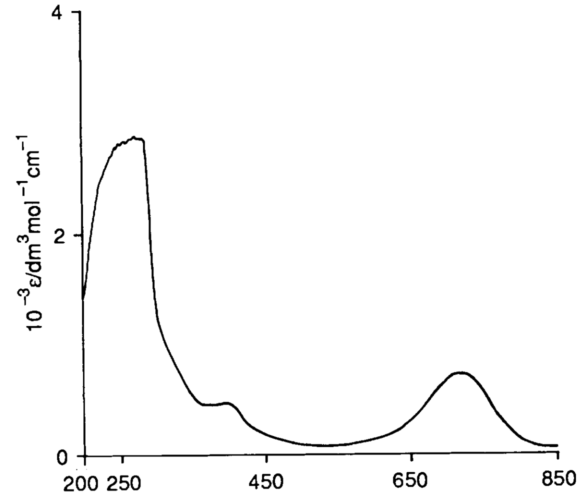

Fig. 6 The UV/VIS spectrum of $[\{Os(NH_3)_4(CH_3CN)\}_2N_2]^{5+}$ in 0.1 mol dm^{-3} HCl

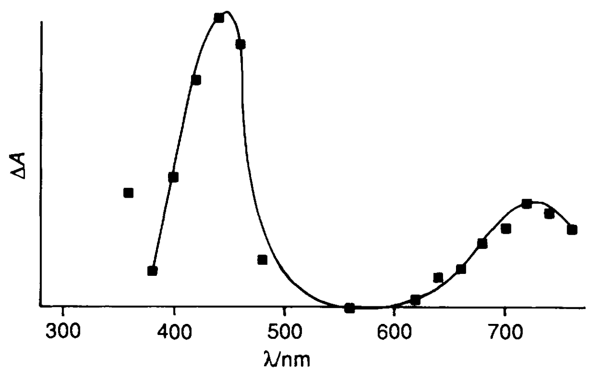

Fig. 7 Transient optical difference spectrum recorded 50 μs after 355 nm laser excitation of $[OsN(NH_3)_4]^{3+}$ (*ca.* 10^{-3} mol dm^{-3}) and 1,4-dimethoxybenzene (*ca.* 10^{-3} mol dm^{-3}) in degassed acetonitrile

Photolysis in the Presence of an Electron Donor.—One of the interesting photochemical properties of nitridoosmium(VI) complexes is the dependence of the emission lifetime on the complex concentration. However, attempts to investigate the self-quenching reaction by laser flash photolysis were unsuccessful. Steady-state photolysis did not lead to any net reaction.

Photolysis of $[OsN(NH_3)_4]^{3+}$ in the presence of an electron donor gave completely different results. With hexamethylbenzene in degassed acetonitrile a green solution was found after photolysis. The spectral changes of the photochemical reaction are shown in Fig. 5. A rapid development of the absorption peak at *ca.* 720 nm was observed. As discussed later this peak started to form *ca.* 20 μs after flashing an acetonitrile solution of $[OsN(NH_3)_4]^{3+}$ and 1,4-dimethoxybenzene or hexamethylbenzene. Evaporation of the solvent after photolysis yielded an air-stable green solid which showed no ν(Os≡N) in the IR spectrum. Its electronic absorption spectrum in water resembles that of the $[\{Os(NH_3)_5\}_2N_2]^{5+}$ complex synthesized by Taube and co-workers.[7] The perchlorate salt of the photolysed product was obtained by redissolving the above green solid in methanol followed by precipitation with excess of $LiClO_4$. A deep green solid was collected and washed with absolute methanol and diethyl ether. The product was recrystallized from dilute hydrochloric acid. X-Ray diffraction studies confirmed the molecular structure of $[\{Os(NH_3)_4(CH_3CN)\}_2N_2][ClO_4]_5$.[1c]

The complex $[\{Os(NH_3)_4(CH_3CN)\}_2N_2]^{5+}$ is stable in the solid and in aqueous solution. Its UV/VIS spectrum in 0.1 mol dm^{-3} HCl (Fig. 6) shows a low-energy absorption band at 720 nm. The IR spectrum shows no ν(N≡N) stretching in the region 2005–2015 cm^{-1}. The kinetic stability and intense visible absorption can be attributed to the extensive electron delocalization among the metal centres. In contrast to the $[Ru^{II}-N_2-Ru^{III}]^{5+}$ unit, where electronic coupling between the metal centres is weak,[13] the mixed-valence $[Os^{II}-N_2-Os^{III}]$ is a strongly interacting system. The very weak or absent ν(N≡N) band in the IR spectrum is also the case with other symmetric osmium μ-dinitrogen species such as $[\{Os(NH_3)_4Cl\}_2N_2]^{3+}$ and $[\{Os(NH_3)_5\}_2]^{5+}$ and is caused by rapid electron delocalization.[13]

Photolysis of $[OsN(NH_3)_4]^{3+}$ in the presence of other electron donors such as 1,4-dimethoxybenzene and diphenylamine gave similar results. Fig. 7 shows the difference absorption spectrum for the photochemical reaction between $[OsN(NH_3)_4]^{3+}$ and 1,4-dimethoxybenzene in acetonitrile recorded 50 μs after flash photolysis. The spectrum is characterized by the peaks at *ca.* 460 and 720 nm. The former is attributed to the formation of the 1,4-dimethoxybenzene cation radical, the latter to formation of the μ-dinitrogen product. Of these transient signals the former was formed instantaneously after the laser flash but decayed at a slower rate, while the latter absorption took *ca.* 100 μs to become fully developed (Fig. 8). The rapid formation of the cation radical and the slow rate of growth of $[Os^{II}-N_2-Os^{III}]$ indicates that they were not produced from the same reaction step. The slow decay rate of

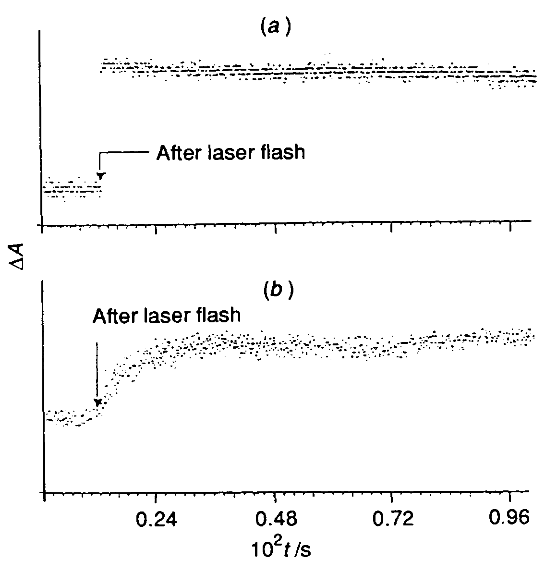

Fig. 8 Growth trace of the transient absorption at (*a*) 460 and (*b*) 720 nm of a $[OsN(NH_3)_4]^{3+}$ (*ca.* 10^{-3} mol dm^{-3}) and 1,4-dimethoxybenzene (*ca.* 10^{-3} mol dm^{-3}) mixture in degassed acetonitrile

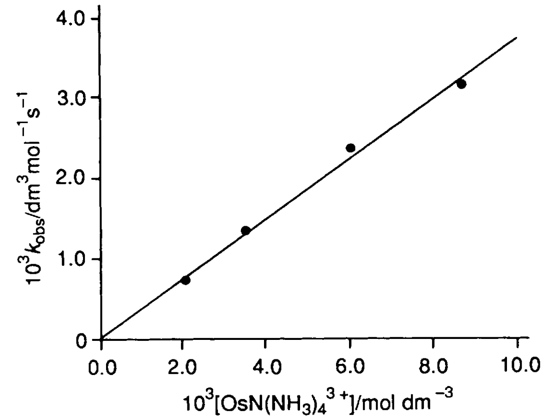

Fig. 9 A plot of the rate constant for the production of $[\{Os(NH_3)_4(CH_3CN)\}_2N_2]^{5+}$ *vs.* concentration of $[OsN(NH_3)_4]^{3+}$

Table 4 Quantum yield of $[\{Os(NH_3)_4(CH_3CN)\}_2N_2]^{5+}$ with various electron donors in degassed acetonitrile[a]

Quencher[b]	E_p/V *vs.* NHE	φ_0[c]	$k_q[Q]/k_{self}[Os{\equiv}N]$
Diphenylamine	1.07	0.345	82.5
Triphenylamine	1.10	0.367	59.6
1,4-Dimethoxybenzene	1.58	0.355	2.19
Hexamethylbenzene	1.82	0.317	2.90
Pentamethylbenzene	1.95	0.224	1.71
1,2,4,5-Tetramethylbenzene	2.03	0.169	0.46
1,2,3-Trimethylbenzene	2.23	0.020	0.04

[a] Concentration of $[OsN(NH_3)_4][CF_3SO_3]_3 = 2.6 \times 10^{-3}$ mol dm^{-3}. [b] Concentration of quencher = 0.022 mol dm^{-3}. [c] At 298 K.

the 1,4-dimethoxybenzene cation radical also indicates that the back electron transfer process is slow, which is expected for a bimolecular event. Coupling of the ground state $[OsN(NH_3)_4]^{3+}$ with the photogenerated $[Os^V{\equiv}N]$ intermediate to form the μ-dinitrogen complex is likely [equation (6)].

$$[Os^V{\equiv}N] + [N{\equiv}Os^{VI}] \longrightarrow [Os^{II}{-}N{\equiv}N{-}Os^{III}] \quad (6)$$

In order to estimate the rate of coupling of $[Os^V{\equiv}N]$ and $[Os^{VI}{\equiv}N]$, the kinetics of the formation of the signal at 720 nm after the laser flash was investigated. Pseudo-first-order kinetics with rate = $k_{obs}[Os^V]$ where $k_{obs} = k_2[Os^{VI}{\equiv}N]$ was observed. A plot of the rate constant for the production of $[Os^{II}{-}N_2{-}Os^{III}]$ (k_{obs}) *vs.* $[OsN(NH_3)_4]^{3+}$ concentration (Fig. 9) reveals the bimolecular coupling rate constant (k_2) to be $(3.75 \pm 0.3) \times 10^5$ dm^3 mol^{-1} s^{-1} at 298 K. This rate constant was found to be independent of the laser energy and the concentration of 1,4-dimethoxybenzene.

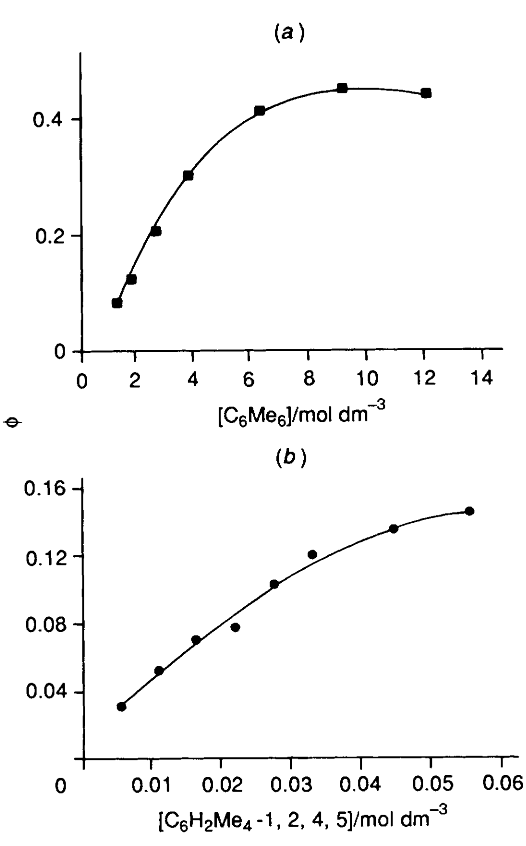

Fig. 10 A plot of φ *vs.* concentration of (*a*) hexamethylbenzene and (*b*) 1,2,4,5-tetramethylbenzene in degassed acetonitrile at 298 K

Quantum Yield Studies of the Formation of $[\{Os(NH_3)_4(CH_3CN)\}_2N_2]^{5+}$.—As the rate constants of the self-quenching and the electron-transfer processes are much larger than that of the coupling reaction, the rate-determining step in the formation of $[\{Os(NH_3)_4(CH_3CN)\}_2N_2]^{5+}$ should be the coupling reaction between $[Os^V{\equiv}N]$ and $[Os^{VI}{\equiv}N]$. However, there is a second pathway competing with the formation of $[Os^V{\equiv}N]$ through electron transfer with an electron donor: the self-quenching process of $[OsN(NH_3)_4]^{3+*}$. The latter pathway will be dominant at low electron donor concentration and high concentration of the $[Os^{VI}{\equiv}N]$ complex.

Table 4 shows the quantum yield (φ) values of $[\{Os(NH_3)_4(CH_3CN)\}_2N_2]^{5+}$ with different organic electron donors in acetonitrile. In cases where the quenching rates with organic quenchers are much larger than the self-quenching rate the quantum yields are similar despite the difference in the oxidation potential of the quenchers. This is consistent with the coupling between $[Os^V{\equiv}N]$ and $[Os^{VI}{\equiv}N]$ being the rate-determining step.

A plot of φ *vs.* the concentration of the quenchers (hexamethylbenzene and 1,2,4,5-tetramethylbenzene) is shown in Fig. 10). For both quenchers a plateau region is observed at high quencher concentration. At low organic quencher concentration self-quenching is expected to be the dominant pathway and only a small quantity of $[OsN(NH_3)_4]^{3+*}$ can be converted into $[Os^V{\equiv}N]$. As the concentration of organic quencher increases more $[Os^V{\equiv}N]$ is produced and φ increases. At the plateau

$$[\mathrm{Os^{VI}{\equiv}N}] \xrightarrow{h\nu} [\mathrm{Os^{VI}{\equiv}N}]^*$$

$$[\mathrm{Os^{VI}{\equiv}N}]^* + [\mathrm{Os^{VI}{\equiv}N}] \rightleftharpoons [\mathrm{Os^{VI}{\equiv}N \cdots N{\equiv}Os^{VI}}]$$

$$[\mathrm{Os^{VI}{\equiv}N \cdots N{\equiv}Os^{VI}}] \rightleftharpoons [\mathrm{Os^{III}{-}N{\equiv}N{-}Os^{III}}] \xrightarrow{\text{reductant}} [\mathrm{Os^{II}{-}N{\equiv}N{-}Os^{III}}]$$

Scheme 1

region the electron-transfer reaction is dominant and the coupling between $[\mathrm{Os^{V}{\equiv}N}]$ and $[\mathrm{Os^{VI}{\equiv}N}]$ becomes the rate-determining step. As the electron-transfer quenching rate constant of 1,2,4,5-tetramethylbenzene is almost seven times smaller than that of hexamethylbenzene, a much higher concentration of the former should be required for the electron-transfer process to mask any self-quenching event. The plateau region is expected to be observed at a higher concentration for 1,2,4,5-tetramethylbenzene, which was the case in this work.

The above studies clearly favour the mechanism described in Scheme 1. An alternative for the formation of the μ-dinitrogen complex involves the interaction of $[\mathrm{OsN(NH_3)_4}]^{3+*}$ with the $[\mathrm{OsN(NH_3)_4}]^{3+}$ ground state to form a μ-dinitrogen diosmium(II) intermediate followed by electron-transfer reaction to produce the $[\mathrm{Os^{II}{-}N_2{-}Os^{III}}]$ complex. However, such a mechanism is disproved by the flash photolysis study.

Disproportionation of $[\{\mathrm{Os(NH_3)_4(CH_3CN)}\}_2\mathrm{N_2}]^{5+}$ *upon Oxidation by* $\mathrm{Ce^{IV}}$.—By the principle of microscopic reversibility, disproportionation of $[\mathrm{Os^{III}{-}N_2{-}Os^{III}}]$ to two $[\mathrm{Os^{VI}{\equiv}N}]$ should be feasible. Oxidation of $[\{\mathrm{Os(NH_3)_5}\}_2\mathrm{N_2}]^{5+}$ by $\mathrm{Ce^{IV}}$ has been studied by Taube and co-workers[14] but no disproportionation product was identified. The major product isolated after the oxidation was $[\mathrm{Os(NH_3)_4(N_2)}]^{2+}$. Rapid aquation of the $[\mathrm{Os^{III}{-}N_2{-}Os^{III}}]$ complex was suggested to be responsible for the observation. In our study of $[\{\mathrm{Os(NH_3)_4(CH_3CN)}\}_2\mathrm{N_2}]^{5+}$ disproportionation has been observed upon oxidation by $\mathrm{Ce^{IV}}$ in aqueous solution despite the instability of the $[\mathrm{Os^{II}{-}N_2{-}Os^{III}}]$ complex in water. Fig. 11 shows the spectral changes of $[\{\mathrm{Os(NH_3)_4(CH_3CN)}\}_2\mathrm{N_2}]^{5+}$ in the presence of $\mathrm{Ce^{IV}}$. The characteristic low-energy absorption band at *ca.* 720 nm diminished rapidly. Subsequent precipitation with hydrochloric acid yielded a bright yellow solid which gave the characteristic emission and absorption spectra of $[\mathrm{OsN(NH_3)_4}]^{3+}$. However, the yield was about 8–10% based on the amount of $[\{\mathrm{Os(NH_3)_4(CH_3CN)}\}_2\mathrm{N_2}]^{5+}$ used. The low yield of the disproportionation product can be attributed to the kinetic competition arising from the aquation of the $[\mathrm{Os^{III}{-}N_2{-}Os^{III}}]$ species. Although the product(s) of $\mathrm{Os^{III}{-}N_2}$ bond rupture could not be analysed due to the presence of excess of $\mathrm{Ce^{IV}}$, the rate of disproportionation of $[\mathrm{Os^{III}{-}N_2{-}Os^{III}}]$ should be comparable to that of $\mathrm{Os^{III}{-}N_2}$ bond breaking since a reasonable quantity of $[\mathrm{OsN(NH_3)_4}]^{3+}$ could be isolated. By selecting suitable ligands and solvent system we expect the aquation process can be suppressed so that the disproportionation reaction will be the dominant reaction.

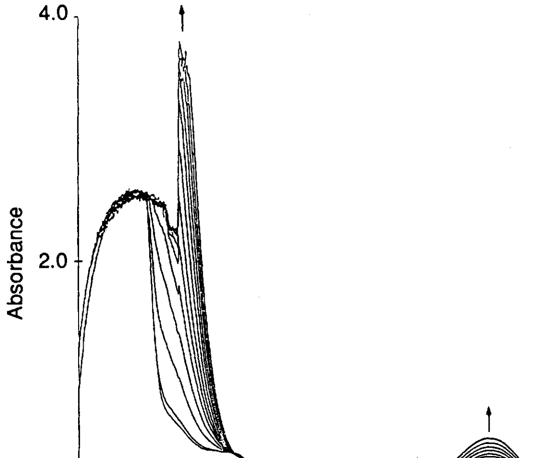

Fig. 11 The UV/VIS spectral changes for the oxidation of $[\{\mathrm{Os(NH_3)_4(CH_3CN)}\}_2\mathrm{N_2}]^{5+}$ by $\mathrm{Ce^{IV}}$ in water at 298 K

Conclusion

The results demonstrate the rich photochemistry of osmium(VI) nitrido complexes. Here, the application of luminescent inorganic metal complexes in the study of the nitrido-coupling reaction is illustrated. Given the observed large bimolecular rate constant for the reaction between $[\mathrm{Os^{V}{\equiv}N}]$ and $[\mathrm{Os^{VI}{\equiv}N}]$, it is not difficult to envisage that the reverse reaction, $\mathrm{M{-}N{\equiv}M{-}M} \longrightarrow 2\ \mathrm{M{\equiv}N}$, could operate at a fast rate by judicious choice of auxiliary ligands.

Acknowledgements

We acknowledge support from the University of Hong Kong, the Croucher Foundation and the Research Council of Hong Kong. H.-W. L. is grateful for a studentship administered by the Croucher Foundation. Drs. K. C. Cho and V. M. Miskowski are thanked for their assistance in laser flash spectroscopic and low-temperature emission measurements.

References

1 (*a*) C. M. Che, T. C. Lau, H. W. Lam and C. K. Poon, *J. Chem. Soc., Chem. Commun.*, 1989, 114; (*b*) C. M. E. Che, H. W. Lam and T. C. W. Mak, *J. Chem. Soc., Chem. Commun.*, 1989, 1529; (*c*) C. M. Che, H. W. Lam, W. F. Tong, T. F. Lai and T. C. Lau, *J. Chem. Soc., Chem. Commun.*, 1989, 1883.
2 V. W. W. Yam and C. M. Che, *New J. Chem.*, 1989, **13**, 707; *Coord. Chem. Rev.*, 1990, **97**, 93.
3 J. R. Winkler and H. B. Gray, *Inorg. Chem.*, 1985, **24**, 346.
4 M. D. Hopkins, V. M. Miskowski and H. B. Gray, *J. Am. Chem. Soc.*, 1986, **108**, 6908.
5 D. D. Perrin and W. L. F. Armarego, *Purification of Laboratory Chemicals*, 3rd edn., Pergamon, Oxford, 1988, ch. 3.
6 J. N. Demas and G. A. Crosby, *J. Phys. Chem.*, 1971, **75**, 991.
7 J. D. Buhr, J. R. Winkler and H. Taube, *Inorg. Chem.*, 1980, **19**, 2416.
8 C. D. Cowman, W. C. Trogler, K. R. Mann, C. K. Poon and H. B. Gray, *Inorg. Chem.*, 1976, **15**, 1747.
9 K. Dehnicke and J. Strahle, *Angew. Chem., Int. Ed. Engl.*, 1981, **20**, 413.
10 R. A. Wheeler, N. H. Whangbo, T. Hughbanks, R. Hoffman, J. K. Burdett and T. A. Albright, *J. Am. Chem. Soc.*, 1986, **108**, 2222.
11 R. Ballardini, G. Varani, M. T. Indelli, F. Scandola and V. Balzani, *J. Am. Chem. Soc.*, 1978, **100**, 7219; J. O. Mowell, J. M. Goncalves, L. Armatore, L. Klasinc, R. M. Wightman and J. K. Kochi, *J. Am. Chem. Soc.*, 1984, **106**, 3968.
12 C. R. Bock, J. A. Connor, A. R. Gutierrez, T. J. Meyer, D. G. Whitten, B. P. Sullivan and J. K. Nagle, *J. Am. Chem. Soc.*, 1979, **101**, 4815.
13 D. E. Richardson, J. P. Sen, J. D. Buhr and H. Taube, *Inorg. Chem.*, 1982, **21**, 3136.
14 P. A. Lay, R. H. Magnuson, H. Taube, J. Ferguson and E. R. Krausz, *J. Am. Chem. Soc.*, 1985, **107**, 2551.

Received 11*th November* 1991; *Paper* 1/05702B